

X-ray and optical plateaus following the main bursts in GRBs and SNe II-P: a hint about similar late injection behaviors? *

Xiao-Hong Cui¹ and Ren-Xin Xu²

¹ National Astronomical Observatories, Chinese Academy of Sciences, Beijing 100012, China;
xhcui@bao.ac.cn

² School of Physics and State Key Laboratory of Nuclear Physics and Technology, Peking University, Beijing 100871, China

Received 2012 May 23; accepted 2013 March 11

Abstract We analyze the emission plateaus in the X-ray afterglow light curves of gamma-ray bursts (GRBs) and those in the optical light curves of type II plateau supernovae (SNe II-P) in order to study whether they have similar late energy injection behaviors. We show that correlations of bolometric energies (or luminosities) between the prompt explosions and the plateaus for the two phenomena are similar. The energy emitted by SNe II-P are at the lower end of the range of possible energies for GRBs. The bolometric energies (or luminosities) in the prompt phase E_{expl} (or L_{expl}) and in the plateau phase E_{plateau} (or L_{plateau}) share relations of $E_{\text{expl}} \propto E_{\text{plateau}}^{0.73 \pm 0.14}$ and $L_{\text{expl}} \propto L_{\text{plateau}}^{0.70}$. These results may indicate a similar late energy injection behavior that produces the observed plateaus in these two phenomena.

Key words: gamma rays: bursts — supernovae: general — methods: statistical

1 INTRODUCTION

One of the major topics for today’s astrophysicists is to understand the explosive mechanisms of gamma-ray bursts (GRBs) and core-collapse supernovae. Very interestingly, a radiation plateau often appears in the X-ray/optical bands of GRBs and a similar optical plateau appears after the initial bursts of type II plateau supernovae (SNe II-P). We focus on this feature and study the possible relations of the plateaus with the initial bursts for these two kinds of events.

On one hand, the early X-ray afterglow of a GRB is found to show a canonical behavior (Zhang et al. 2006; Nousek et al. 2006) that can be observed by the X-Ray Telescope (XRT) on *Swift*. As one of the components in this canonical X-ray light curve, the shallow decay phase, i.e. “plateau,” typically lasts a few thousand seconds with a temporal decay slope ~ -0.5 . Various kinds of models, such as the energy injection model (Rees & Meszaros 1998; Nousek et al. 2006; Zhang et al. 2006), the reverse shock model (Genet et al. 2007), the two component model (de Pasquale et al. 2009), the dust scattering model (Shao & Dai 2007) etc, have been proposed to explain this enigmatic phase. However, a chromatic behavior, where no optical break or spectral evolution occurs during the transition time (t_{tr}) from the plateau to the normal decay phase in more than half of the bursts (Fan &

* Supported by the National Natural Science Foundation of China.

Piran 2006; Liang et al. 2007), is very difficult to interpret within the framework of the external shock models (Fan & Piran 2006; Panaitescu et al. 2006). Suppressed forward shock emission is required for long lasting reverse shock models (Genet et al. 2007; Uhm & Beloborodov 2007). The spectral evolution could not be interpreted by the effect of dust scattering (Shao & Dai 2005) though the light curve can be explained. Also, the two-component external shock jets (de Pasquale et al. 2009) would require contrived shock parameters. A long-lasting central engine therefore possibly explains the X-ray plateau phase in GRB afterglow emission and is related to the chromatic scenario (Liang et al. 2007). From the observations, the isotropic X-ray energy ($E_{\text{iso,X}}$) for the plateau phase in the afterglow of a GRB is found to be correlated with the prompt gamma-ray energy and the transition time t_{tr} (Liang et al. 2007). An anti-correlation has been found between the end time of the plateau T_{a} and the X-ray luminosity (L_{X}) at T_{a} in the rest frame of the GRB (Dainotti et al. 2010). By adding a third parameter, the isotropic γ -ray energy E_{iso} , Xu & Huang (2012) found a new and significantly tighter three-parameter correlation for GRBs with a plateau phase in the afterglow.

On the other hand, plateaus also appear in the light curves of SNe II-P. Observationally, SNe II-P are classified as a “plateau” due to the slow decay of their early light curves (Barbon et al. 1979), where the luminosity remains nearly constant for a period of ~ 70 –100 days (Pskovskii 1978). Their expansion velocities, plateau luminosities and durations show a wide range (Young & Branch 1989; Hamuy 2001). In order to reproduce the plateaus of SNe II-P, a red supergiant progenitor with an extensive hydrogen envelope would be necessary (Grassberg et al. 1971; Falk & Arnett 1977). An analytic model (Arnett 1980; Popov 1993) and hydrodynamic models (Litvinova & Nadezhin 1983, 1985) have been introduced to explain the light curves of SNe II-P and their correlation with the physical parameters of progenitor stars. It is conventionally accepted that the plateau phase in SNe II-P results from the recombination of ionized hydrogen. However, the way that photons diffuse through the expanding envelope after the shock reaches the surface and the mechanism of energy deposition in the envelope is still unknown, though much effort has been made to study the structure and the hydrodynamic processes in the envelope after the core collapse of the central star (Arnett 1980; Popov 1993; Litvinova & Nadezhin 1983, 1985; Burrows et al. 2006; Janka et al. 2007; Utrobin & Chugai 2009).

It is known that some long GRBs are associated with core-collapse SNe. The discovery of 30 associations between long, soft GRBs and Type Ib/c SNe (see, e.g., the review by Woosley & Bloom 2006 and Hjorth & Bloom 2012) directly indicates that their progenitors are massive stars. These associations have resulted in finding common explosive processes for SNe and GRBs to form rapidly spinning black holes (Woosley 1993), neutron stars (Kluźniak & Ruderman 1998) or even quark stars (Dai & Lu 1998a). A quantitative relation between the peak spectral energy of a GRB and the peak bolometric luminosity of an SN was also presented to clarify that the critical parameter determining the GRB-SN connection is the peak luminosity of SNe (Li 2006). In the standard collapsar model of GRBs, collimation of the outflow is essential for avoiding baryon loading and producing a clean fireball. However, for some GRBs/X-ray flashes (XRFs), the jet opening angle inferred from the correlation between the jet opening angle of GRBs and the peak energy of their spectra measured in the GRB frame is so large that the burst outflow should be spherical (Li 2006). This is consistent with radio observations of soft XRF 020903, GRB 060218 and XRF 080109 (Soderberg et al. 2004, 2006, 2008). Two possible scenarios for producing a GRB/XRF from a spherical configuration have been presented (Li 2008).

Comparative studies of plateaus in GRB afterglows and those in SNe II-P can reveal their properties, hydrodynamics and the possible physical process/origins. The goal of this work is to show the implications of a correlation for the plateau phenomena and a similar hydrodynamical process or energy injection behavior during the plateau phase. In this paper, we analyze the observed parameters for 43 *Swift* XRT GRB afterglows and those for 11 SNe II-P collected from prior work. A correlation between the energies E_{expl} in the prompt phase and E_{plateau} ($L_{\text{plateau}} \times \tau$, where τ is the duration of the plateau phase) in the plateau phase has been found for both samples. The relation between the

luminosities $L_{\text{expl}} (E_{\text{expl}}/\tau)$ and L_{plateau} can also be well fitted with a power law. The power-law indices of both correlations are found to be similar for two samples within the error bar ranges. This may imply a similarity between the dynamic processes or energy injection behaviors that produce the plateaus during these two kinds of explosions of GRB afterglow and SNe II-P, though in different regimes. The energy budgets for plateau and (prompt) explosion are correlated for both samples, respectively. The data of samples and the calculation method are presented in Section 2. The bolometric luminosity is deduced from the fitting of the light curve for GRB X-ray afterglows and SNe II-P. In order to compare the properties of the plateau, in Section 3 we present two correlations between the luminosities L_{expl} and L_{plateau} , as well as the energies E_{expl} and E_{plateau} , for GRB and SNe II-P samples. The results are summarized in Section 4 with some discussion.

2 DATA AND METHOD

The X-ray afterglow of our GRB sample is downloaded from the *Swift* XRT data archive. The redshifts of the bursts in this GRB sample are all detected up to 2010 December, and the sample includes only those XRT light curves with a clear initial steep decay segment, a shallow decay segment and a normal decay segment detected by *Swift*/XRT. We compile a sample of 43 GRBs including the 33 GRBs in the work of Cui et al. (2010) and another 10 bursts after 2008 November as shown in Table 1. From this table, we can find that the values for redshift in our GRB sample are in the range 0.42 (GRB 050803) to 5.11 (GRB 060522) and the mean value of redshift for these 43 bursts is about 2.3. The starting time (t_1) and the midpoint flux (f_p) of the plateau segment are obtained by fitting the steep-to-shallow decay segment with a smoothed broken power law function (Cui et al. 2010). The end time of this segment (t_2) is taken as the break time between the plateau and normal decay phase. The duration of the plateau is then $\tau_{\text{GRB}} = t_2 - t_1$. With redshift z , the luminosity distance (D_L) of the burst can be obtained by adopting cosmological parameters $\Omega_M = 0.3$, $\Omega_\Lambda = 0.7$ and $H_0 = 71 \text{ km s}^{-1} \text{ Mpc}^{-1}$. Thus, the luminosity at the midpoint of the plateau phase of the GRB X-ray afterglow can then be calculated by

$$L_{\text{plateau,GRB}} = 4\pi\kappa_X \times D_L^2 \times f_p. \quad (1)$$

Assuming the emission in the plateau phase from the source is mainly from the observed band, the factor κ_X corrects the flux at the observed energy band ($[E_1, E_2]$ in units of keV) of an instrument (XRT here, i.e., $[E_1=0.3 \text{ keV}, E_2=10 \text{ keV}]$) to that at a band $(0.01 - 100)/(1+z)$ keV, which is

$$\kappa_X = \frac{\int_{0.01/(1+z)}^{100/(1+z)} E\Phi(E)dE}{\int_{E_1}^{E_2} E\Phi(E)dE}, \quad (2)$$

where $\Phi(E) \propto E^{-\Gamma_X}$ and Γ_X (as shown in Table 1) is the photon index for the photon spectrum (Dainotti et al. 2010). The error of $L_{\text{plateau,GRB}}$ is deduced by the errors of the best fitting parameters for the plateau phase based on the error transfer formula.

As the opening angles for most GRBs in our sample are not known and the explosion of an SN is thought to be almost isotropic, here we take the gamma-ray isotropic energy of a GRB as the total energy of a GRB in the prompt explosion phase with observed fluence S and redshift z ,

$$E_{\text{expl,GRB}} = 4\pi\kappa_\gamma D_L^2 S/(1+z). \quad (3)$$

The factor κ_γ is applied to convert the observed fluence at the observational energy band of an instrument (from E_1 to E_2 , in units of keV) to that at a standard band $(1 - 10^4)/(1+z)$ keV in the rest frame of the GRB (Bloom et al. 2001), which reads

$$\kappa_\gamma = \frac{\int_{1/(1+z)}^{10^4/(1+z)} EN(E)dE}{\int_{E_1}^{E_2} EN(E)dE}, \quad (4)$$

Table 1 Properties of the GRB Sample

GRB	z	T_{90} (s)	Γ_X	τ_{GRB} (ks)	$L_{\text{plateau,GRB}}$ ($10^{48} \text{erg s}^{-1}$)	$E_{\text{expl,GRB}}$ (10^{53}erg)
050416A	0.65	2.4	2.15	0.17 ± 0.11	0.07 ± 0.05	0.01
050803	0.42	110	1.88	1.24 ± 0.09	0.03 ± 0.02	0.03
050908	3.35	19.4	3.9	0.52 ± 0.14	0.27 ± 0.87	0.35
051016B	0.94	4	2.82	6.85 ± 2.31	0.02 ± 0.01	0.01
051109A	2.346	14.3	2.33	0.58 ± 0.14	3.59 ± 1.50	0.90
060108	2.03	14.4	1.91	2.23 ± 0.74	0.12 ± 0.10	0.12
060210	3.91	255	1.93	0.59 ± 0.15	15.70 ± 5.08	6.91
060418	1.49	103.1	2.04	0.06 ± 0.02	3.03 ± 1.28	1.57
060502A	1.51	33	2.43	5.12 ± 1.51	0.18 ± 0.06	0.45
060510B	4.9	275.2	1.42	13.41 ± 3.25	0.07 ± 0.19	5.05
060522	5.11	71.1	1.97	0.05 ± 0.02	6.13 ± 31.03	1.50
060526	3.21	298.2	1.8	1.11 ± 0.28	0.53 ± 0.56	0.85
060605	3.8	79.1	1.6	0.58 ± 0.15	2.06 ± 3.17	0.6
060607A	3.08	100	1.79	1.20 ± 0.02	11.61 ± 3.33	1.61
060707	3.43	66.2	2	0.64 ± 0.16	1.08 ± 1.34	1.19
060708	2.3	9.8	2.51	0.59 ± 0.38	0.61 ± 0.40	0.20
060714	2.71	15	2.02	0.53 ± 0.10	1.49 ± 1.28	1.47
060729	0.54	116	2.71	6.95 ± 0.30	0.03 ± 0.01	0.07
060814	0.84	146	1.84	1.64 ± 0.17	0.07 ± 0.05	0.94
060906	3.68	43.6	2.44	1.31 ± 0.33	0.60 ± 0.45	1.83
061121	1.31	81	1.62	1.90 ± 0.44	1.11 ± 0.18	2.04
070110	2.35	85	2.11	2.13 ± 0.04	0.78 ± 0.40	0.67
070306	1.497	209.5	2.29	1.63 ± 0.39	0.28 ± 0.21	1.02
070318	0.836	74.6	1.4	0.10 ± 0.04	0.24 ± 0.58	0.16
070721B	3.626	340	1.48	0.64 ± 0.16	5.51 ± 5.93	2.91
071021	5	225	2.12	1.81 ± 0.43	0.60 ± 1.08	1.66
080310	2.4266	365	2.85	1.73 ± 0.43	0.41 ± 0.53	1.00
080430	0.767	16.2	2.42	0.71 ± 0.17	0.05 ± 0.02	0.06
080607	3.036	79	1.68	0.08 ± 0.02	27.49 ± 15.53	14.85
080707	1.23	27.1	1.81	0.61 ± 0.15	0.04 ± 0.04	0.07
080905B	2.374	128	1.49	0.50 ± 0.12	7.05 ± 72.07	0.75
081007	0.5295	10	3	1.20 ± 0.28	0.02 ± 0.01	0.02
081008	1.9685	185.5	1.91	1.06 ± 0.26	0.64 ± 0.37	1.32
090529	2.625	>100	2.5	2.59 ± 0.65	0.05 ± 0.14	0.34
090618	0.54	113.2	2.11	0.66 ± 0.16	0.48 ± 0.07	2.79
090927	1.37	2.2	1.64	1.15 ± 0.33	0.03 ± 0.07	0.03
091029	2.752	39.2	2	1.19 ± 0.29	0.56 ± 0.36	1.27
100302A	4.813	17.9	2.28	5.17 ± 1.23	0.23 ± 0.26	0.38
100418A	0.624	7	4.29	8.80 ± 2.08	0.002 ± 0.001	0.01
100621A	0.542	63.6	2.15	1.33 ± 0.32	0.08 ± 0.04	0.56
100704A	3.6	197.5	2.6	1.10 ± 0.27	3.36 ± 1.27	4.80
100814A	1.44	174.5	1.9	14.45 ± 3.38	0.26 ± 0.08	1.60
100906A	1.727	114.4	2.15	0.69 ± 0.17	1.33 ± 0.72	2.94

where E is photon energy and $N(E)$ is the band function defined by Band et al. (1993). Since it is difficult to derive the spectral index for individual GRBs from only BAT observations in a narrow energy band, mean spectral indices $\alpha \simeq -1$, $\beta \simeq -2.2$ and peak energy values $E_p \simeq 250$ keV obtained are substituted into the $N(E)$ formula (Preece et al. 2000).

For type II SNe, three physical parameters, explosion energy $E_{\text{expl,SN}}$, envelope mass and initial radius, are mainly determined by the outburst properties, the plateau duration τ in the light curve, the absolute V magnitude M_V at the midpoint of the plateau phase, and the material velocity u_{ph} at the photosphere. With these three observed parameters, Litvinova & Nadezhin (1983; 1985, LN85 hereafter) presented three approximation formulae to calculate the three physical parameters mentioned above based on the hydrodynamical models. We collect the observed SNe II-P data with explosion

Table 2 Properties of the SN II-P Sample

SN	cz (km s^{-1})	τ_{SN} (d)	$L_{\text{plateau,SN}}$ ($10^{41} \text{ erg s}^{-1}$)	$E_{\text{expl,SN}}$ (10^{51} erg)	Reference
1991al	4484	90	20.6	2.61	[1, 7]
1992af	5438	90	12.5	2.46	[1, 7]
1992ba	1165	100	7.5	0.57	[1, 7]
1999br	1292	100	1.5	0.2	[1, 7]
1999cr	6376	100	9.7	0.9	[1, 7]
1999em	669	120	8	0.84	[1, 8]
1999gi	592	115	6.7	0.64	[2, 8]
2003gd	657	113	7.8	1.04	[3, 8]
2004dj	132	105	7.4	0.65	[4, 8]
2004et	48	110	10.1	0.88	[5, 8]
2005cs	463	118	3.1	0.17	[6, 8]

References: [1] Hamuy (2001); [2] Nakano & Kushida (1999); [3] Carnegie Type II Supernovae Survey (CATS); [4] Vinko et al. (2006); [5] Zwitter et al. (2004); [6] Kloehr et al. (2005); [7] Nadyozhin (2003); [8] Maguire et al. (2010).

energy $E_{\text{expl,SN}}$ and the bolometric luminosity at the midpoint of the plateau phase $L_{\text{plateau,SN}}$. This bolometric luminosity for our SNe II-P sample comes from the work of Bersten & Hamuy (2009, BH09 hereafter). They derived calibrations for bolometric corrections and effective temperature from *BVI* photometry and obtained the bolometric light curve for a sample of 33 SNe II-P. Within this sample, only 11 SNe with the observed parameters have explosion energy $E_{\text{expl,SN}}$ that was calculated in the prior work (Nadyozhin 2003; Maguire et al. 2010). Our SN II-P sample is composed of these 11 SNe and their properties are presented in Table 2.

In BH09's sample, the zero point of time was taken as the midpoint between the plateau and the radioactive tail. We also take this zero point as the end of the plateau phase in this work. A smoothed broken power law is then used to fit the light curve for the data with $t < 0$

$$L = L_0 \left[\left(\frac{t}{t_p} \right)^{\omega\alpha_1} + \left(\frac{t}{t_p} \right)^{\omega\alpha_2} \right]^{-1/\omega}, \quad (5)$$

where L_0 is the normalization parameter for the fitting. Parameter ω describes the sharpness of the break and t_p is the time representing the beginning point of the plateau. α_1 and α_2 denote the slopes of components before plateau and during plateau, respectively. The duration of the plateau τ_{SN} and the bolometric luminosity at the midpoint of the plateau $L_{\text{plateau,SN}}$ can be obtained by the best fitting parameters with $\tau_{\text{SN}} = |t_p|$ and $L_{\text{plateau,SN}} = L(t_p/2) = L_0(2^{-\omega\alpha_1} + 2^{-\omega\alpha_2})^{-1/\omega}$.

3 RESULTS

The properties of the GRB sample from the observations and the parameters deduced from the formulae, as described by Equations (1) to (4), are presented in Table 1: the redshift z , the duration of the prompt phase T_{90} , photon index in the afterglow phase Γ_X , the duration of the plateau τ_{GRB} , the bolometric luminosity at the midpoint of the plateau $L_{\text{plateau,GRB}}$, and the value of energy in the prompt phase $E_{\text{expl,GRB}}$. Table 2 lists the properties of 11 SNe II-P included in this study. The selection standards for our SNe II-P sample are these SNe II-P with (1) the measurement of the plateau duration (as shown in Column 3 of Table 2); (2) the bolometric corrections for the light curves (e.g. BH09), and then the bolometric luminosity $L_{\text{plateau,SN}}$ at the midpoint of the plateau phase (as shown in Column 4 of Table 2); (3) the absolute V magnitude M_V at the plateau; (4) the material velocity u_{ph} in the photosphere at the midpoint of the plateau. Based on the parameters described by (1), (3) and (4), the explosion energy $E_{\text{expl,SN}}$ (as shown in Col. (5) of Table 2) can be obtained by applying the hydrodynamical models that are presented by LN85.

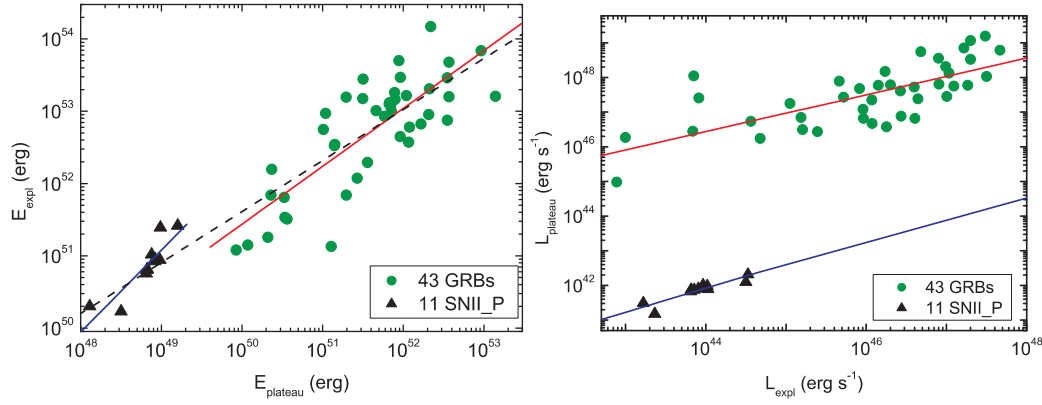


Fig. 1 Correlation diagram of bolometric luminosities and energies at the midpoint of plateau phase and prompt phase for GRB and SNe II-P samples. The red and blue lines are the best linear fits for GRB and SNe II-P samples, respectively. *Left panel*: The relation between energies E_{expl} in the prompt phase and those in the plateau phase E_{plateau} , the dashed line is the best fitting for both samples. *Right panel*: The relation between the luminosities L_{plateau} and L_{expl} .

Table 3 Fitting Results for GRB and SN II-P Samples

Correlation	Sample	Slope	r^a	SD^b	p^c
$E_{\text{expl}}-E_{\text{plateau}}$	GRB	0.80 (0.09)	0.81	0.47	$< 10^{-4}$
	SN II-P	1.13 (0.20)	0.89	0.18	2.93×10^{-4}
	SN II-P + GRB	0.73 (0.14)	0.91	0.43	$< 10^{-4}$
$L_{\text{plateau}}-L_{\text{expl}}$	GRB	0.79 (0.07)	0.88	0.44	$< 10^{-4}$
	SN II-P	0.69 (0.11)	0.91	0.14	1.26×10^{-4}

a: Spearman correlation coefficient; *b*: Standard deviation; *c*: Chance probability.

The left panel of Figure 1 shows the correlation of E_{plateau} with E_{expl} for GRB X-ray afterglow and SNe II-P samples. The right panel of this figure presents the relation of luminosities L_{plateau} and L_{expl} (i.e. E_{expl}/τ). A linear fit is applied to test the correlations for each sample on a logarithmic scale and fitting results are presented in Table 3. From this table and Figure 1, we can find that E_{plateau} (i.e. $\tau \times L_{\text{plateau}}$) and E_{expl} as well as L_{plateau} and L_{expl} are correlated for the two samples, respectively. All the Spearman correlation coefficients r are larger than 0.8 with chance probabilities $p \sim 10^{-4}$. This implies that the prompt isotropic gamma-ray energy is indeed correlated with the isotropic X-ray energy in the plateau phase (Liang et al. 2007) and the energy budgets for the plateau phase and the (prompt) explosion energy are correlated for both samples. The slopes in the $E_{\text{expl}}-E_{\text{plateau}}$ diagram on the logarithmic scale for two linear fittings are 0.80 ± 0.09 and 1.13 ± 0.20 . For the sample (SNe II-P+GRBs), it is 0.73 ± 0.14 . Thus we can find that all of the slopes, which are the power law indices of the linear terms, are very near each other. The slopes of the correlation $L_{\text{plateau}}-L_{\text{expl}}$ on the logarithmic scale are also found to be very close, 0.79 ± 0.07 and 0.69 ± 0.11 for GRB and SN II-P samples, respectively. Thus it is possible that the processes of energy injection to the shock/ejected material in the (prompt) explosion and in the plateau phase are very similar.

The gap (~ 2.23) in the vertical direction between the best fitting lines of the two samples in the $L_{\text{plateau}}-L_{\text{expl}}$ diagram might indicate different ways or levels of energy being injected by

explosions during the X-ray plateau for GRB afterglows and the (prompt) plateau for SNe II-P. That is to say, the central engine or energy budgets of GRBs and SNe II-P during the plateaus could be different. The energy deposited into the ejecta or circumburst materials for GRBs is larger than that for SNe II-P during the plateau phases. Therefore, the plateaus for the two samples would appear in different observational energy bands. GRBs exhibit these emissions in the X-ray band but SNe II-P show them in the optical band. The very near power law indices of best fittings for GRB and SN II-P samples considering the error bars may indicate that the hydrodynamic process or the energy injection behavior, e.g. the shockwave propagation in the circumburst materials during the plateau phase for GRBs and SNe II-P, could be very similar.

4 CONCLUSIONS AND DISCUSSION

By comparing the plateaus in the light curves of GRB X-ray afterglows and in the explosion phase of SNe II-P, we find that the (prompt) explosion energy E_{expl} and the energy in the plateau phase E_{plateau} are correlated, and the luminosity L_{plateau} and L_{expl} are also correlated. All the Spearman correlation coefficients for the linear fittings in $E_{\text{expl}}-E_{\text{plateau}}$ and $L_{\text{plateau}}-L_{\text{expl}}$ diagrams on a logarithmic scale are larger than 0.8 with chance probabilities $p \sim 10^{-4}$. This implies that the energy injected in the (prompt) explosion and plateau phases are correlated for GRBs and SNe II-P, respectively. The similar power indices of the best fittings for the two samples may indicate similar hydrodynamic processes during the energy injection that occurs in the plateau phases. The gap in the $L_{\text{plateau}}-L_{\text{expl}}$ diagram between two best fitting lines might imply that the central engine or the way energy is deposited into the ejecta of the two samples could be different.

The optical data of GRB afterglow have been collected by Li et al. (2012). An optical shallow-decay segment in these GRB afterglows was observed in 39 GRBs. Based on their results, a rough proportionality between the isotropic energy in the prompt phase $E_{\gamma,\text{iso}}$ and isotropic R -band energy $E_{R,\text{iso}}$ in the optical shallow-decay segment is observed in their work. The best fitting between these two quantities is $\log E_{R,\text{iso}} = 0.40 + 0.47 \log E_{\gamma,\text{iso}}$ with chance probability $p \sim 6 \times 10^{-3}$. The isotropic energy $E_{\gamma,\text{iso}}$ is the same as the energy E_{expl} in the prompt phase as presented in Equation (3) in this work. Compared with the fitting slopes shown in Table 3, we can find that the correlation between $E_{R,\text{iso}}$ and $E_{\gamma,\text{iso}}$ is different from that of E_{plateau} and E_{expl} in this work.

The very origin of plateaus is quite difficult to identify though it is very likely to be related to the external shock (e.g. Zhang 2007). However, the spectral index generally does not change across the temporal break (Liang et al. 2007) from the plateau phase to the following decay phase. Thus the models invoking a radiation mechanism can be ruled out for the origin of the plateau phase. A hydrodynamical or geometrical origin is proposed by Zhang (2007). The dynamics associated with continuous injection were discussed by invoking a spin-down pulsar (Dai & Lu 1998a,b; Zhang & Mészáros 2001) with a smoothly varying luminosity $L \propto t^{-q}$ (Zhang & Mészáros 2001) and a value $q \sim 2$ is suggested by the observational data (Fan & Xu 2006; Rowlinson et al. 2010). Alternatively, the GRB plateau may be due to the solidification of quark stars (Xu & Liang 2009; Dai et al. 2011), which favor clean fireballs without baryon contamination (Paczynski & Haensel 2005; Chen et al. 2007).

The hydrodynamical process of envelope ejection is also one of the characteristic features of SNe II-P. Litvinova & Nadezhin (1983, 1985) presented a series of hydrodynamical models of SNe II-P and found that the light curves were determined by the size and mass of the progenitor's unstable envelope. The usual hypothesis about the SNe explosion can be decoupled into the collapse of the core and the ejection of the envelope (e.g. Grassberg et al. 1971, Woosley 1988). These two parts are independent and the observations are only determined by the propagation process of the shock wave produced from the core collapse through the envelope (Falk & Arnett 1977; Bersten et al. 2011). If the process of shock wave propagation in the envelope is the same as that of the external shock involving a GRB afterglow plateau, the hydrodynamics of the energy injection about the plateau

phenomena may be similar for GRB afterglows and SNe II-P samples. The timescale of the similar, underlying hydrodynamical processes and energy that is deposited from the central object could be different because they are possibly determined by the time and amount of energy injected from the central engine, and thus it is possible that the plateaus for GRB afterglows and for SNe II-P emit in different energy bands.

Acknowledgements We would like to thank useful discussions at our pulsar group of PKU. This work is supported by the National Basic Research Program of China (973 program, Grant Nos. 2012CB821800 and 2009CB824800) and the National Natural Science Foundation of China (Grant Nos. 11225314, 11103026 and 10935001).

References

- Arnett, W. D. 1980, *ApJ*, 237, 541
- Band, D., Matteson, J., Ford, L., et al. 1993, *ApJ*, 413, 281
- Barbon, R., Ciatti, F., & Rosino, L. 1979, *A&A*, 72, 287
- Bersten, M. C., & Hamuy, M. 2009, *ApJ*, 701, 200
- Bersten, M. C., Benvenuto, O., & Hamuy, M. 2011, *ApJ*, 729, 61
- Bloom, J. S., Frail, D. A., & Sari, R. 2001, *AJ*, 121, 2879
- Burrows, A., Livne, E., Dessart, L., Ott, C. D., & Murphy, J. 2006, *New Astron. Rev.*, 50, 487
- Chen, A., Yu, T., & Xu, R. 2007, *ApJ*, 668, L55
- Cui, X.-H., Liang, E.-W., Lv, H.-J., Zhang, B.-B., & Xu, R.-X. 2010, *MNRAS*, 401, 1465
- Dai, Z. G., & Lu, T. 1998a, *Physical Review Letters*, 81, 4301
- Dai, Z. G., & Lu, T. 1998b, *A&A*, 333, L87
- Dai, S., Li, L., & Xu, R. 2011, *Science in China G: Physics and Astronomy*, 54, 1541
- Dainotti, M. G., Willingale, R., Capozziello, S., Fabrizio Cardone, V., & Ostrowski, M. 2010, *ApJ*, 722, L215
- de Pasquale, M., Evans, P., Oates, S., et al. 2009, *MNRAS*, 392, 153
- Falk, S. W., & Arnett, W. D. 1977, *ApJS*, 33, 515
- Fan, Y., & Piran, T. 2006, *MNRAS*, 369, 197
- Fan, Y.-Z., & Xu, D. 2006, *MNRAS*, 372, L19
- Genet, F., Daigne, F., & Mochkovitch, R. 2007, *MNRAS*, 381, 732
- Grassberg, E. K., Imshennik, V. S., & Nadyozhin, D. K. 1971, *Ap&SS*, 10, 28
- Hamuy, M. A. 2001, *Type II supernovae as distance indicators*, Ph. D. thesis, The University of Arizona
- Hjorth, J., & Bloom, J. S. 2012, in *Gamma-Ray Bursts, The Gamma-Ray Burst - Supernova Connection*, Cambridge Astrophysics Series 51, eds. C. Kouveliotou, R. A. M. J. Wijers, & S. Woosley (Cambridge Univ. Press), 169
- Janka, H.-T., Langanke, K., Marek, A., Martínez-Pinedo, G., & Müller, B. 2007, *Phys. Rep.*, 442, 38
- Kloehr, W., Muendlein, R., Li, W., et al. 2005, *IAUC*, 8553, 1
- Kluźniak, W., & Ruderman, M. 1998, *ApJ*, 505, L113
- Li, L., Liang, E.-W., Tang, Q.-W., et al. 2012, *ApJ*, 758, 27
- Li, L.-X. 2006, *MNRAS*, 372, 1357
- Li, L.-X. 2008, in *American Institute of Physics Conference Series*, 1065, eds. Y.-F. Huang, Z.-G. Dai, & B. Zhang, 273
- Liang, E.-W., Zhang, B.-B., & Zhang, B. 2007, *ApJ*, 670, 565
- Litvinova, I. I., & Nadezhin, D. K. 1983, *Ap&SS*, 89, 89
- Litvinova, I. Y., & Nadezhin, D. K. 1985, *Soviet Astronomy Letters*, 11, 145
- Nakano, S., & Kushida, R. 1999, *IAUC*, 7329, 1
- Maguire, K., Di Carlo, E., Smartt, S. J., et al. 2010, *MNRAS*, 404, 981
- Nadyozhin, D. K. 2003, *MNRAS*, 346, 97

- Nousek, J. A., Kouveliotou, C., Grupe, D., et al. 2006, *ApJ*, 642, 389
- Paczynski, B., & Haensel, P. 2005, *MNRAS*, 362, L4
- Panaitescu, A., Mészáros, P., Burrows, D., et al. 2006, *MNRAS*, 369, 2059
- Popov, D. V. 1993, *ApJ*, 414, 712
- Preece, R. D., Briggs, M. S., Mallozzi, R. S., et al. 2000, *ApJS*, 126, 19
- Pskovskii, I. P. 1978, *Soviet Ast.*, 22, 201
- Rees, M. J., & Meszaros, P. 1998, *ApJ*, 496, L1
- Rowlinson, A., O'Brien, P. T., Tanvir, N. R., et al. 2010, *MNRAS*, 409, 531
- Shao, L., & Dai, Z. G. 2005, *ApJ*, 633, 1027
- Shao, L., & Dai, Z. G. 2007, *ApJ*, 660, 1319
- Soderberg, A. M., Kulkarni, S. R., Berger, E., et al. 2004, *ApJ*, 606, 994
- Soderberg, A. M., Kulkarni, S. R., Nakar, E., et al. 2006, *Nature*, 442, 1014
- Soderberg, A. M., Berger, E., Page, K. L., et al. 2008, *Nature*, 453, 469
- Uhm, Z. L., & Beloborodov, A. M. 2007, *ApJ*, 665, L93
- Utrobin, V. P., & Chugai, N. N. 2009, *A&A*, 506, 829
- Vinkó, J., Takáts, K., Sárneczky, K., et al. 2006, *MNRAS*, 369, 1780
- Woosley, S. E. 1988, *ApJ*, 330, 218
- Woosley, S. E. 1993, *ApJ*, 405, 273
- Woosley, S. E., & Bloom, J. S. 2006, *ARA&A*, 44, 507
- Xu, M., & Huang, Y. F. 2012, *A&A*, 538, A134
- Xu, R., & Liang, E. 2009, *Science in China G: Physics and Astronomy*, 52, 315
- Young, T. R., & Branch, D. 1989, *ApJ*, 342, L79
- Zhang, B., & Mészáros, P. 2001, *ApJ*, 552, L35
- Zhang, B., Fan, Y. Z., Dyks, J., et al. 2006, *ApJ*, 642, 354
- Zhang, B. 2007, *ChJAA (Chin. J. Astron. Astrophys.)*, 7, 1
- Zwitter, T., Munari, U., & Moretti, S. 2004, *IAUC*, 8413, 1